

Supporting Information for

An analysis of translation distance of tropical cyclones over the western North Pacific

Licheng Wang^{1,2}, Xihui Gu^{1,3,4*}, Aminjon Gulakhmadov^{5,6}, Jianfeng Li⁷, Louise J. Slater⁴, Qiang Zhang^{8,9,10*}, Ming Luo¹¹, Guoyu Ren^{1,12}, Dongdong Kong^{1,3}, Yangcheng Lai⁷, Jianyu Liu¹²

1. Department of Atmospheric Science, School of Environmental Studies, China University of Geosciences, Wuhan 430074, China;
2. CMA-NJU Joint Laboratory for Climate Prediction Studies, School of Atmospheric Sciences, Nanjing University, Nanjing 210023, China;
3. Centre for severe weather and climate and hydro-geological hazards, Wuhan 430074, China;
4. School of Geography and the Environment, University of Oxford, Oxford OX1 3QY, UK;
5. Research Center of Ecology and Environment in Central Asia, Xinjiang Institute of Ecology and Geography, Chinese Academy of Sciences, Urumqi 830011, China;
6. Institute of Water Problems, Hydropower and Ecology of the National Academy of Sciences of Tajikistan, Dushanbe 734042, Tajikistan;
7. Department of Geography, Hong Kong Baptist University, Hong Kong, China;
8. Key Laboratory of Environmental Change and Natural Disaster, Ministry of Education, Beijing Normal University, Beijing 100875, China;
9. Faculty of Geographical Science, Academy of Disaster Reduction and Emergency Management, Ministry of Education/Ministry of Civil Affairs, Beijing Normal University, Beijing 100875, China;
10. State Key Laboratory of Earth Surface Processes and Resources Ecology, Beijing Normal University, Beijing 100875, China;
11. School of Geography and Planning and Guangdong Key Laboratory for Urbanization and Geo-simulation, Sun Yat-Sen University, Guangzhou 510275, China;

12. Laboratory for Climate Studies, National Climate Center, China Meteorological Administration, Beijing 100081, China;
13. Hubei Key Laboratory of Critical Zone Evolution, School of Geography and Information Engineering, China University of Geosciences, Wuhan, China.

*Corresponding authors:

E-mail addresses: guxh@cug.edu.cn (X. Gu) and zhangq68@bnu.edu.cn (Q. Zhang).

This file includes 19 figures and 3 tables.

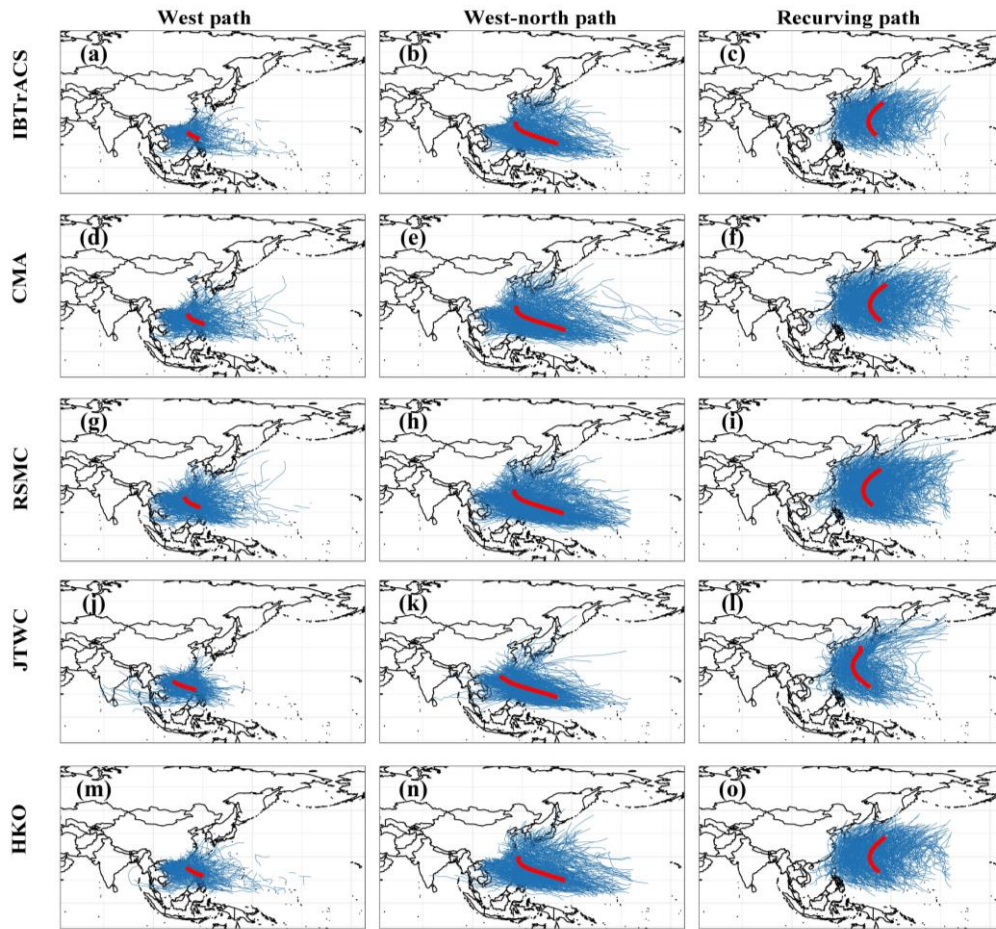


Fig. S1 Tropical cyclone (TC) paths of three categories (i.e. west, west-north, and recurving) over the western North Pacific (WNP) during 1961-2019 using the K-means clustering method. Rows show the classification results based on IBTrACS, CMA, RSMC, JTWC, and HKO datasets, respectively. The red lines indicate the mean path of each category in the three datasets. The mean path is estimated based on the method proposed by Shen et al. (2018).

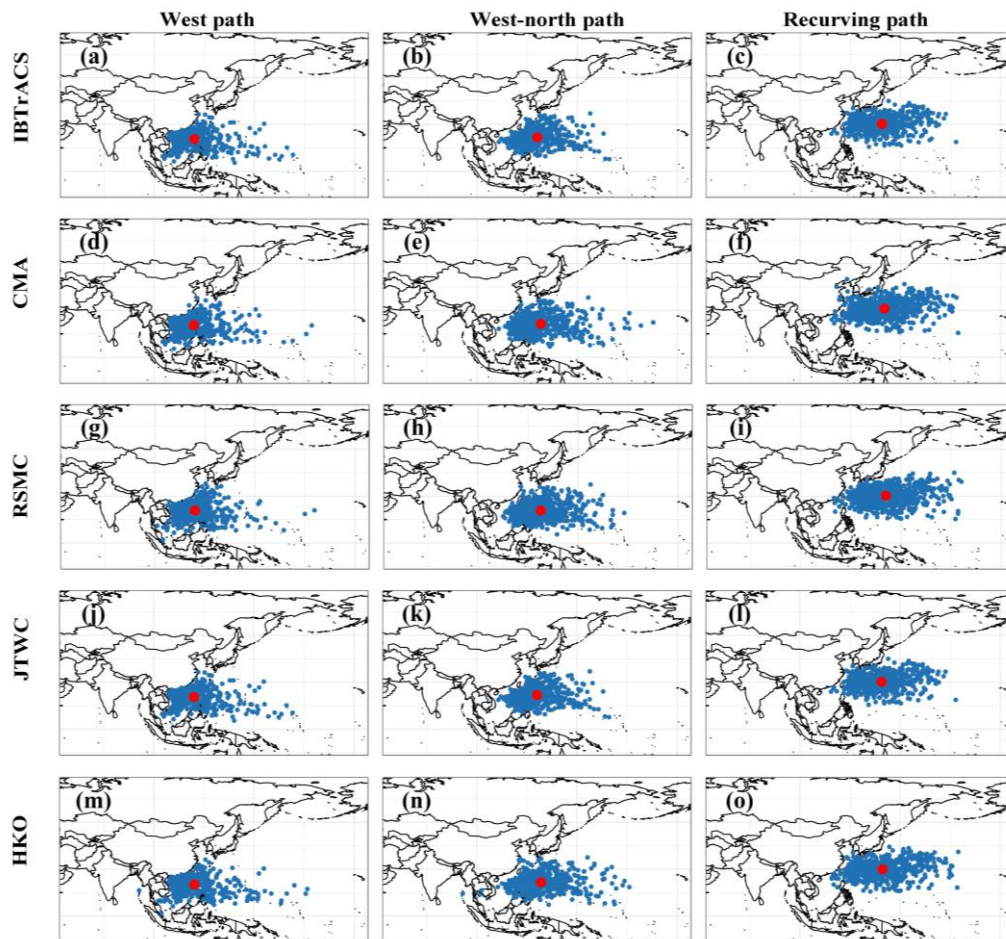


Fig. S2 The same as Fig. S1, but for TC centroid points. The red dots indicate the mean centroid of each category in the three datasets.

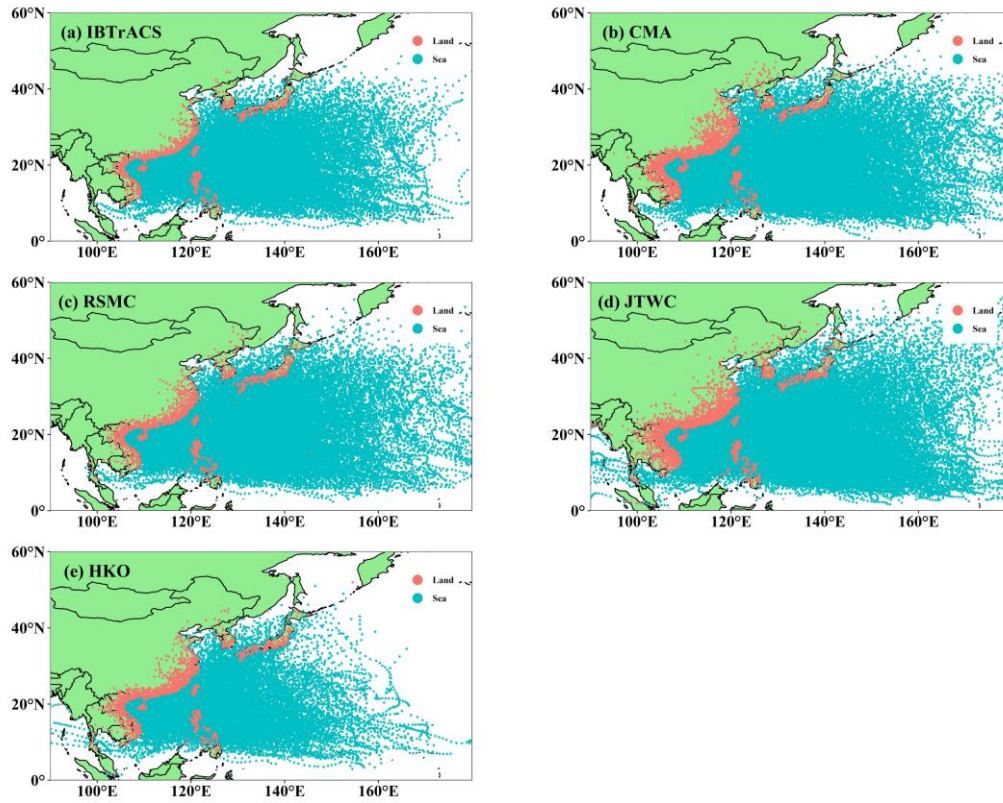


Fig. S3 Spatial distributions of over-land and over-sea TC positions in the five datasets. These TC positions experience the processing of TC best tracks (see Section 3.1 in the main text).

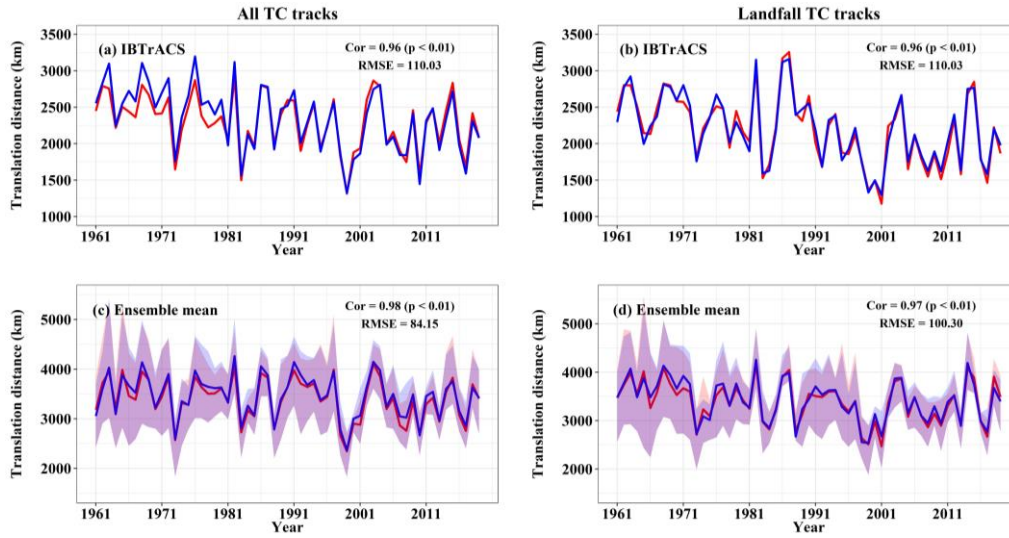


Fig. S4 Annual-mean translation distance of TCs (estimated by D_i and \tilde{D}_i) over the WNP during 1961-2019: a and b are for all and landfalling TCs from the IBTrACS dataset; and c and d are the same as a and b, but for ensemble mean of four TC datasets from CMA, JTWC, RSMC, and HKO, respectively. In c and d, the shadings indicate the fluctuation range of TC translation distance in the four TC datasets. The red and blue lines are the ensemble mean of TC translation distance in D_i and \tilde{D}_i , respectively. “Cor” indicates the Spearman rank correlation between D_i and \tilde{D}_i ; and RMSE indicates the root-mean-square error between D_i and \tilde{D}_i .

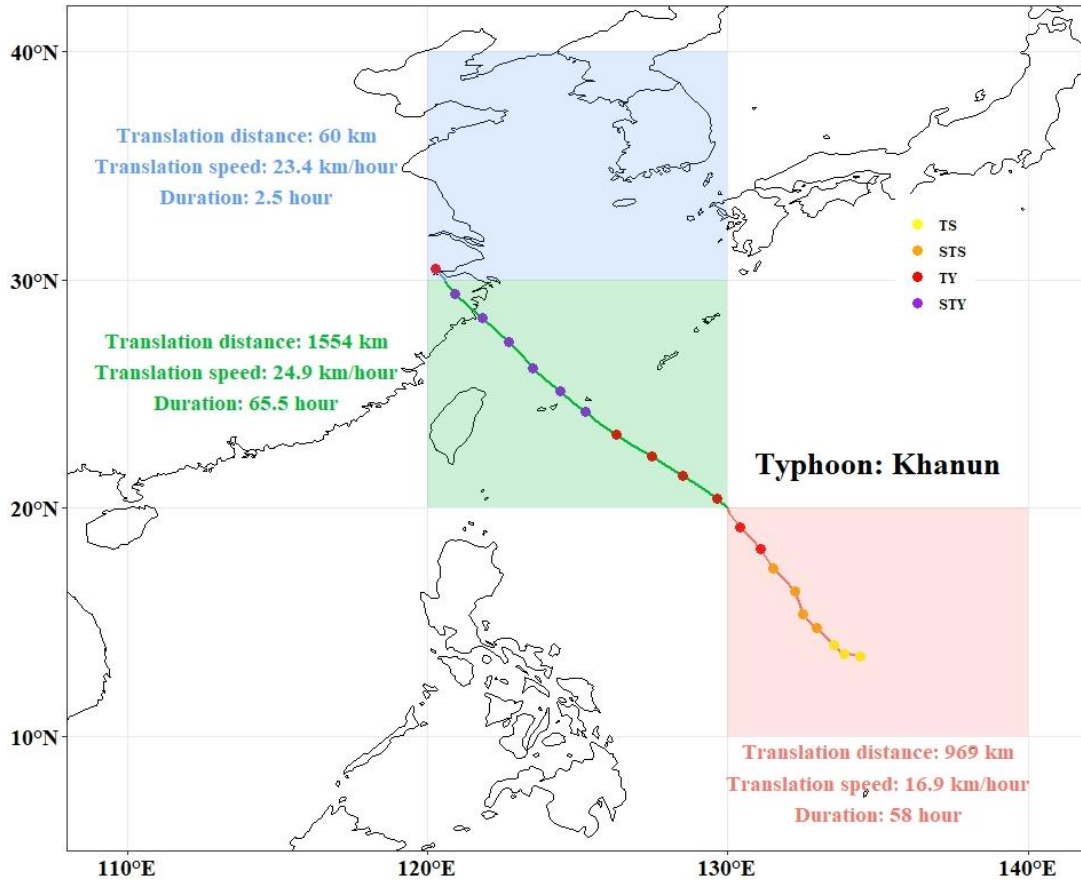


Fig. S5 An example (Typhoon Khanun; see the below Table S1 for more details about this typhoon) to show how to calculate translation distance, duration, and translation speed in each $10^\circ \times 10^\circ$ grid. The TC points are recorded every six hours, and each six-hour interval between two TC positions is a segment. The key issue is that how to deal with TC segments which span two $10^\circ \times 10^\circ$ grids (\square). Taking the TC segment spanning the middle and light green grid, and the upper and light blue grid as an example, we split this TC segment into two parts: one part in the middle grid and the other in the upper grid. The TC translation distances of this TC segment in the two parts are calculated (i.e. 84 km in the middle grid and 60 km in the upper grid), respectively. Assuming that the TC duration is proportional to the TC translation distance in one six-hour TC segment, we then estimate the TC duration of this segment in the two parts (i.e. $6 \times \frac{60}{60+84} = 2.5$ hours in the upper grid and 3.5 hours in the middle grid), respectively. We believe this approach to deal with TC segments spanning two grids can minimize the estimation bias of TC duration and translation distance.

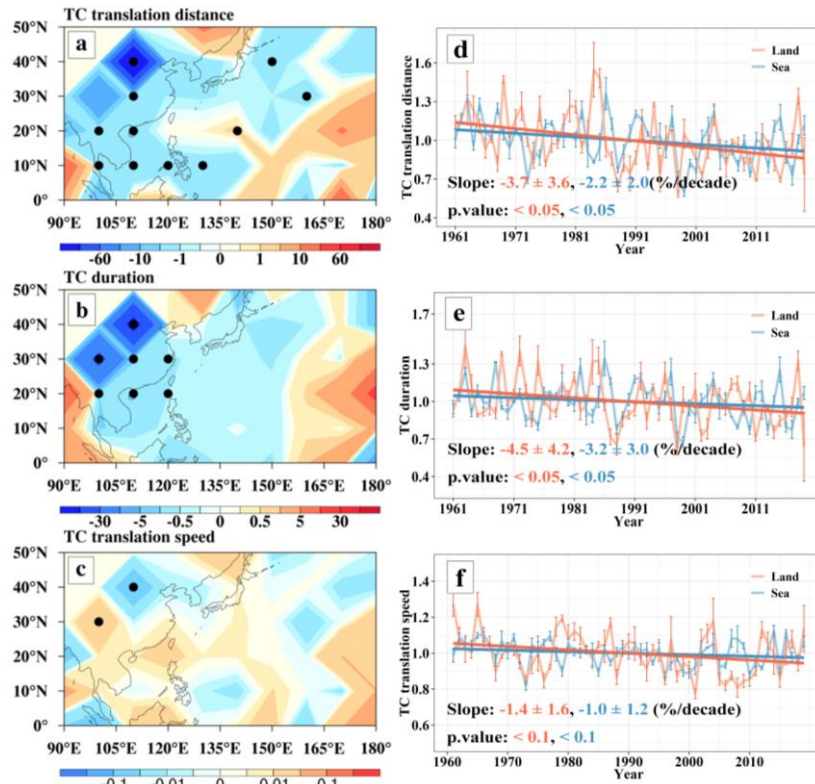


Fig. S6 Spatio-temporal changes in TC translation distance (km per decade), duration (hours per decade), and translation speed (km/hour per decade) of WNP TCs during 1961–2019 from ensemble mean of the four TC datasets (i.e. CMA, RSMC, JTWC, and HKO). In a, b, and c, the locations of TC centers are binned into $10^\circ \times 10^\circ$ grids; annual-mean TC translation distance, duration and translation speed are calculated in each grid, and their trends are detected grid by grid. The stippling in a, b, and c indicates that the trends are significant at the 90% confidence level. For d, e, and f, the annual-mean TC translation distance, duration and translation speed are averaged and then normalized over the land and sea for the entire region separately; error bars indicate the 1 standard error of annual-mean values.

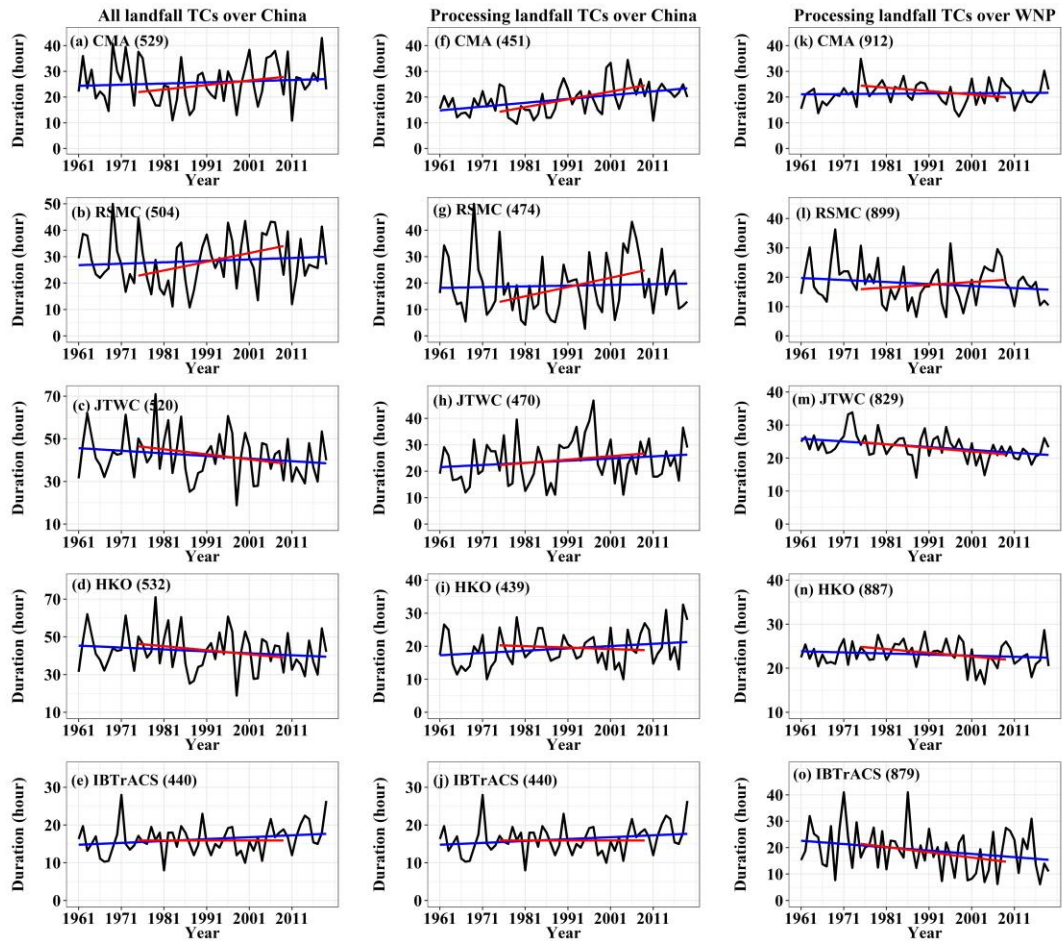


Fig. S7 Over-land duration of TCs that made landfall over China and the WNP. In the left column, TCs landfalling China include tropical depression; in the middle column, TCs landfalling China exclude tropical depression. The number in the bracket in each panel is the total TC count considered during 1961-2019. The right column is the same as the middle column but for landfalling TCs over WNP. The blue line indicates the linear trend during 1961-2019, while the red line for 1975-2009 (the same period as Chen et al. (2011)).

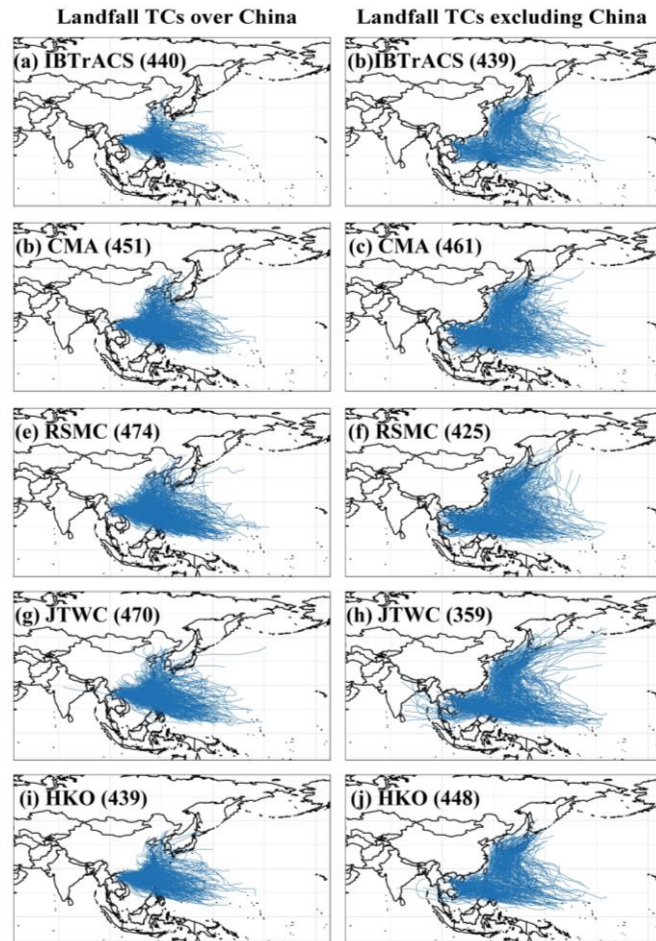


Fig. S8 Landfall TC paths over China (Group 1; the left column) and excluding China (Group 2; the right column) during 1961-2019. Rows show the classification results based on IBTrACS, CMA, RSMC, JTWC, and HKO datasets, respectively.

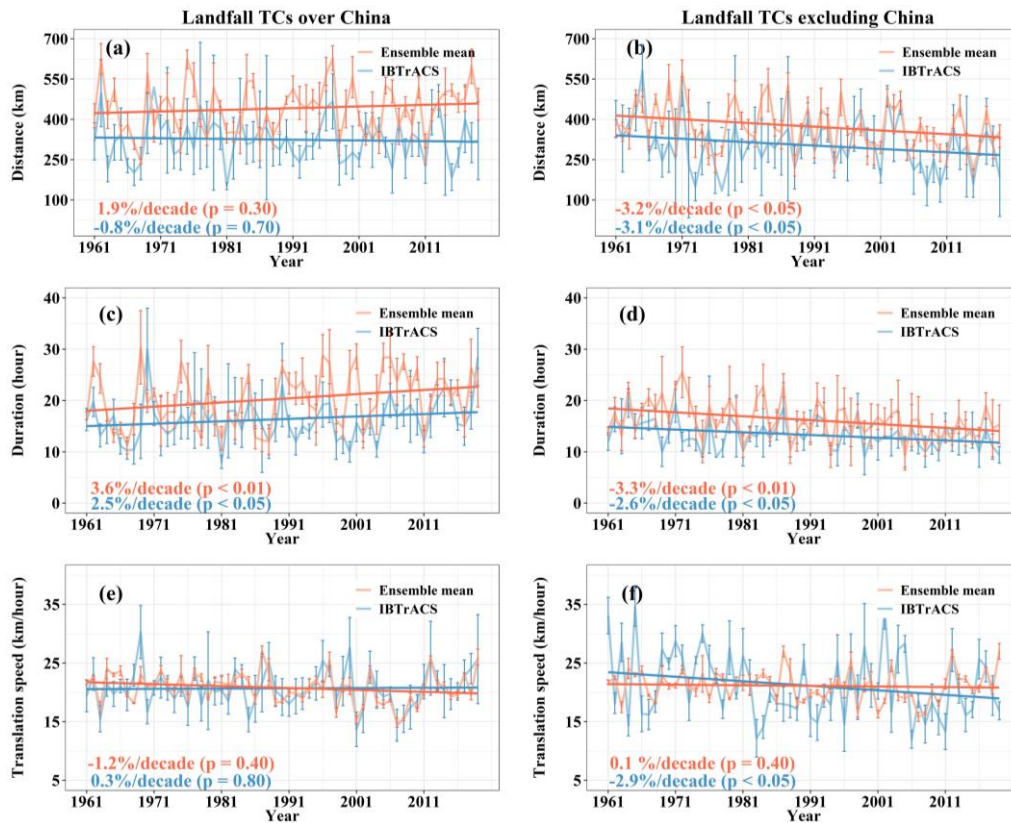


Fig. S9 Temporal changes in over-land translation distance (km per decade), duration (hours per decade), and translation speed (km/hour per decade) of landfall TCs over China (Group 1, left column of Fig. S8) and landfall TCs excluding China (Group 2, right column of Fig. S8) from the IBTrACS dataset (blue) and ensemble mean of four TC datasets from CMA, JTWC, RSMC, and HKO (red), respectively. Error bars indicate the 1 standard error of 1 standard error of annual-mean values.

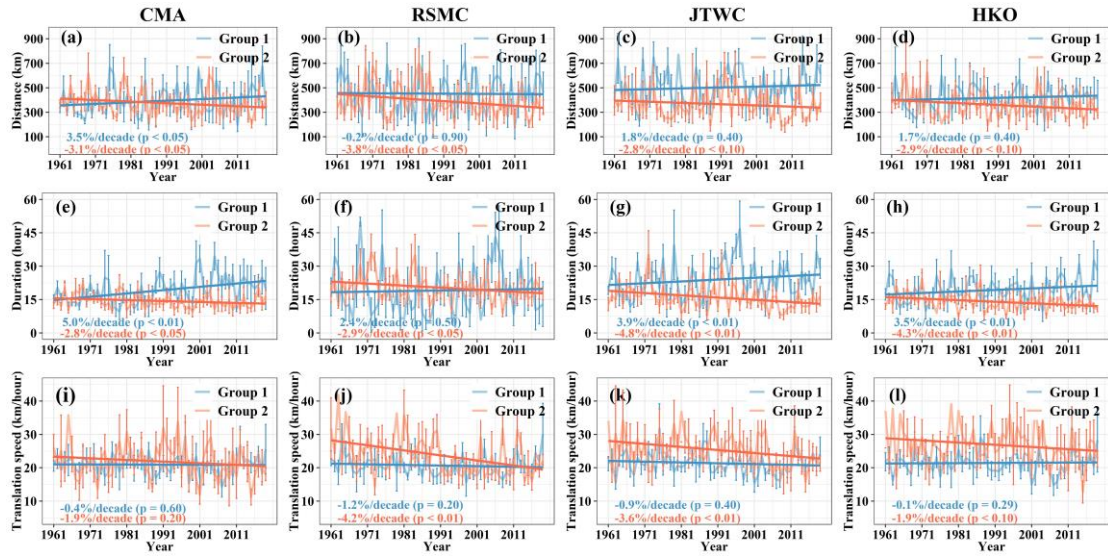


Fig. S10 Temporal changes in over-land translation distance (km per decade), duration (hours per decade), and translation speed (km/hour per decade) of landfall TCs over China (Group 1, left column of Fig. S8) and landfall TCs excluding China (Group 2, right column of Fig. S8) from the four TC datasets (i.e. CMA, JTWC, RSMC, and HKO), respectively. Error bars indicate the 1 standard error of 1 standard error of annual-mean values.

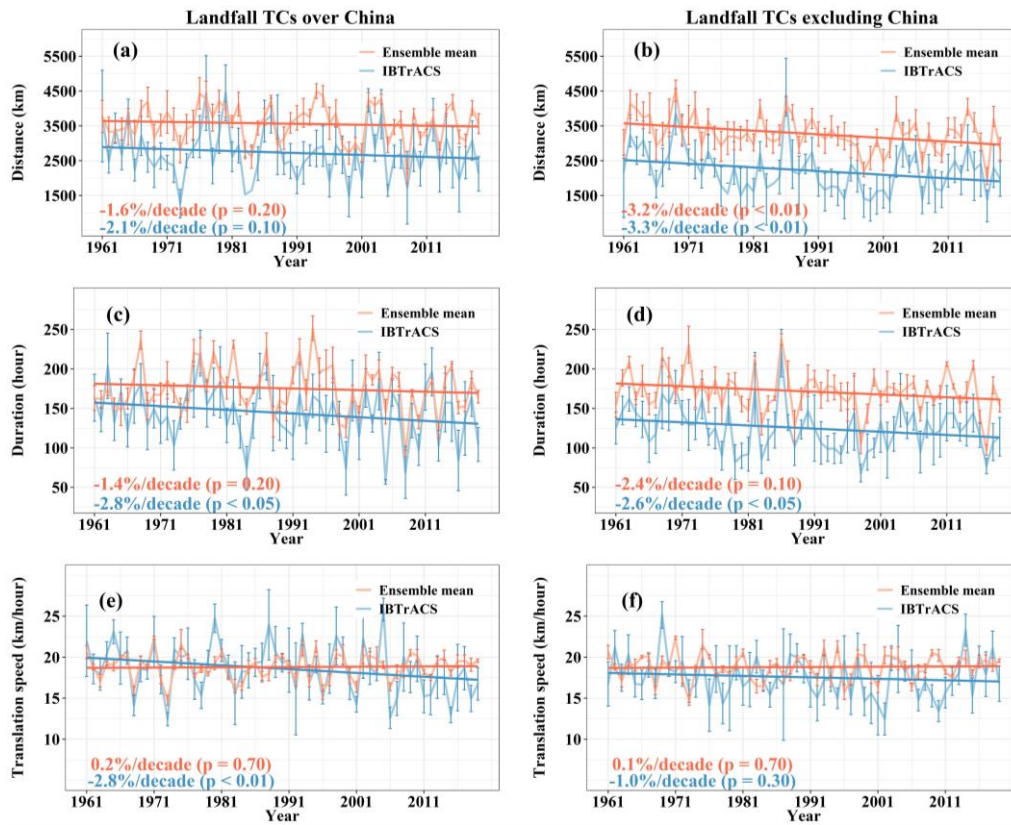


Fig. S11 The same as Fig. S9 but for the translation distance (km per decade), duration (hours per decade), and translation speed (km/hour per decade) from the genesis to the demise (see Section 3.1 in the main manuscript) of landfall TCs.

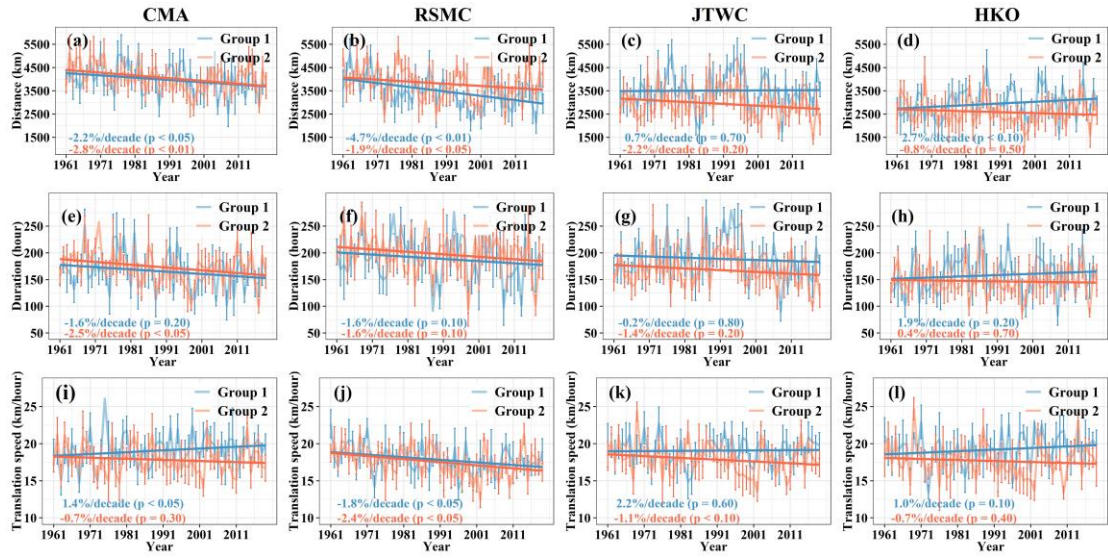


Fig. S12 The same as Fig. 10 but for the translation distance (km per decade), duration (hours per decade), and translation speed (km/hour per decade) from the genesis to the demise (see Section 3.1 in the main manuscript) of landfall TCs.

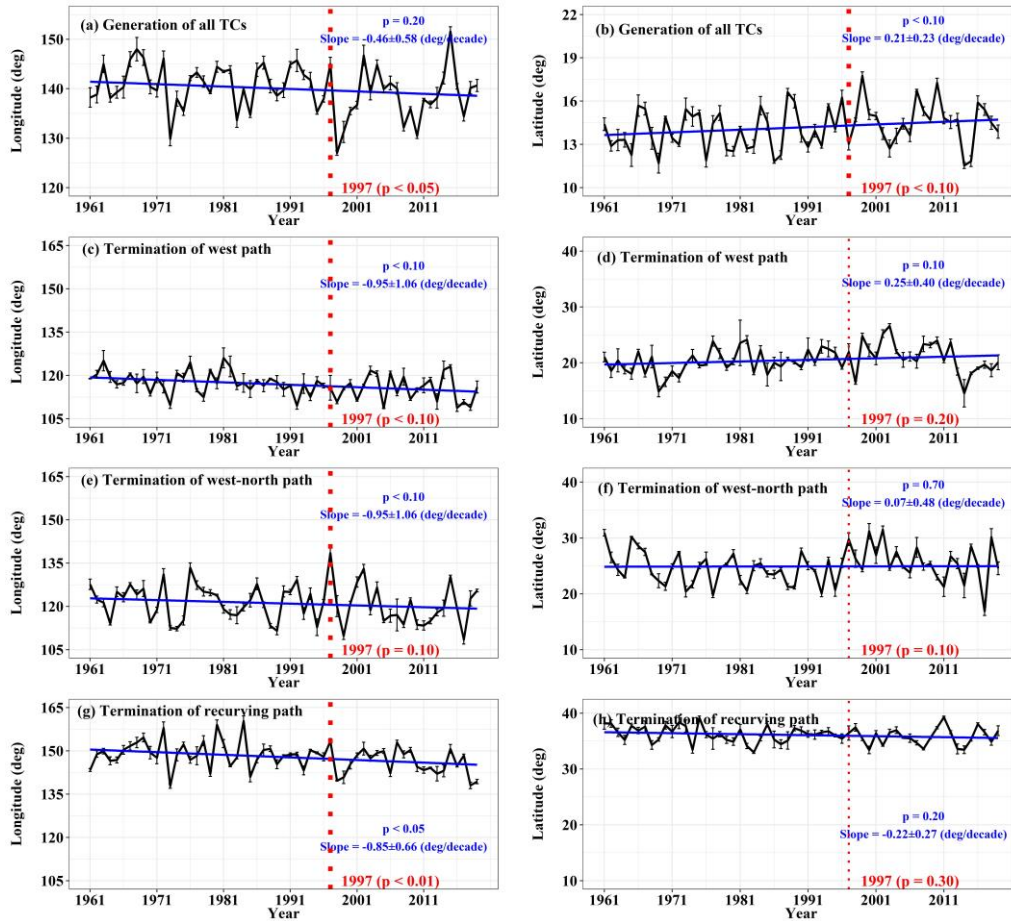


Fig. S13 Temporal changes in location (i.e. longitude and latitude) of TC generations and terminations over the WNP during 1961-2019 from the multi-dataset ensemble mean. Error bars indicate the 1 standard error of annual-mean values. The vertical red dashed lines indicate whether there is an abrupt change point in the year 1997.

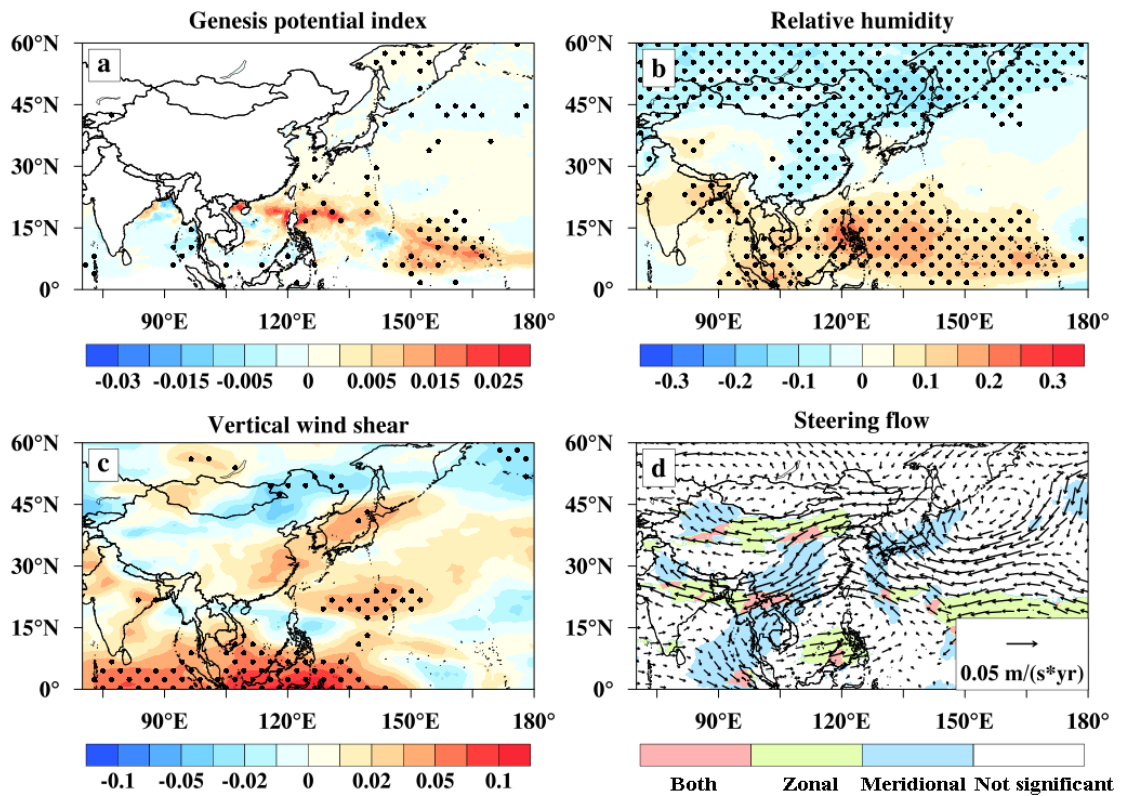


Fig. S14 Long-term trends in genesis potential index (a, per decade), relative humidity (b, % per decade), vertical wind shear (c, m/s per decade), and steering flow (d; zonal and meridional components, arrows, m/s per decade) during 1961-2019. Values are calculated by averaging the variable on all days of TC lifetime in each year. The stippling indicates the long-term trends are significant at the 90% confidence level. In d, the colored shadow indicates the significance of difference in zonal (meridional) steering flow: “Both” indicates the significant in both zonal and meridional steering flow, “Zonal”/“Meridional” indicates the significant in only zonal/ meridional steering flow, and “Not significant” indicates the significant in neither zonal nor meridional steering flow.

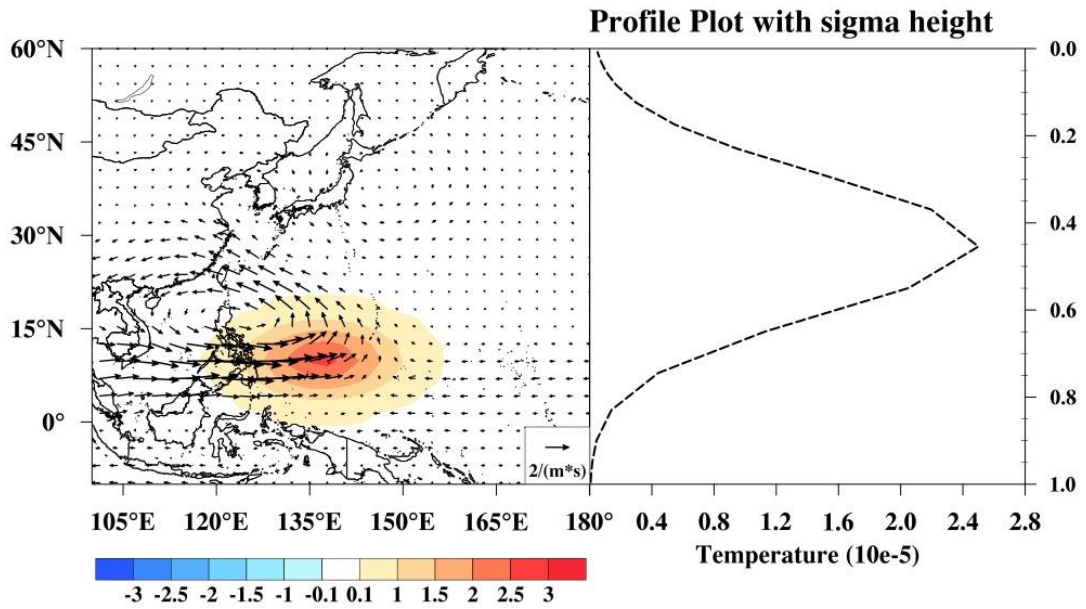


Fig. S15 Heat perturbation of the Linear Baroclinic Model (LBM): the color shading in left column is the spatial distribution of the heat perturbation; 500-hPa wind vectors in the left column are the linear atmospheric responses to the prescribed ideal diabatic heating; and the right column is the vertical profile of diabatic heating.

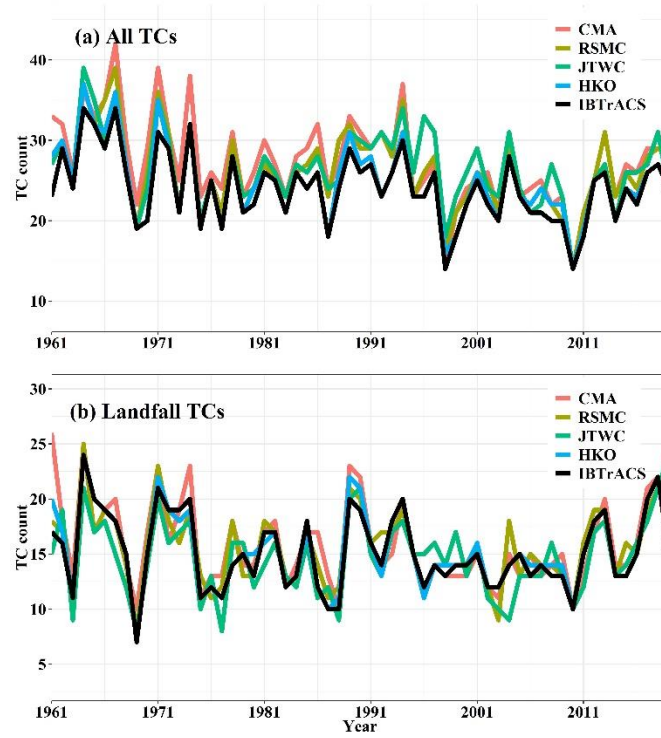


Fig. S16 The year-to-year number of all and landfall TCs over WNP during 1961-2019.

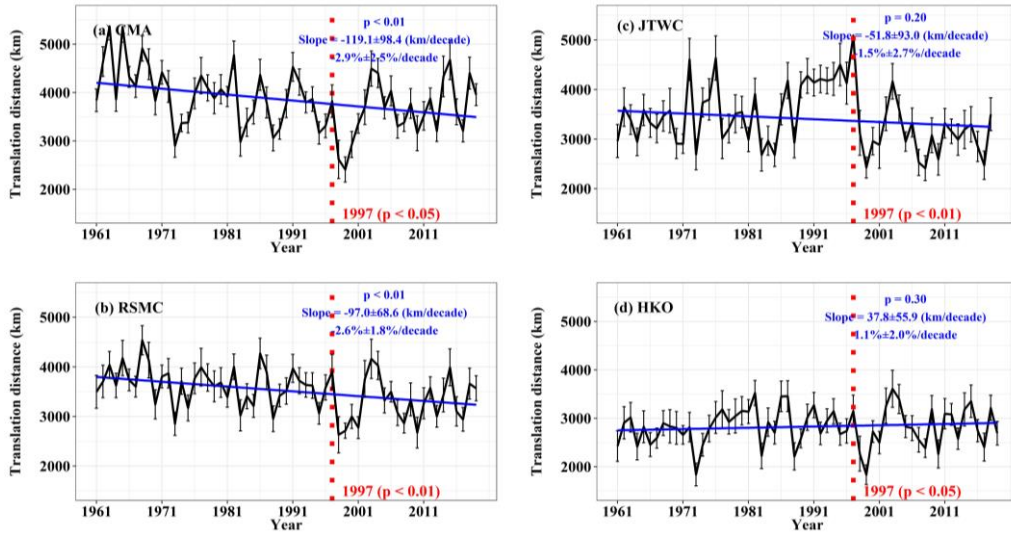


Fig. S17 Temporal changes in the annual-mean translation distance of TCs in the CMA, RSMC, JTWC, and HKO datasets over the western North Pacific (WNP) during 1961-2019, respectively. Error bars indicate the 1 standard error of annual-mean values.

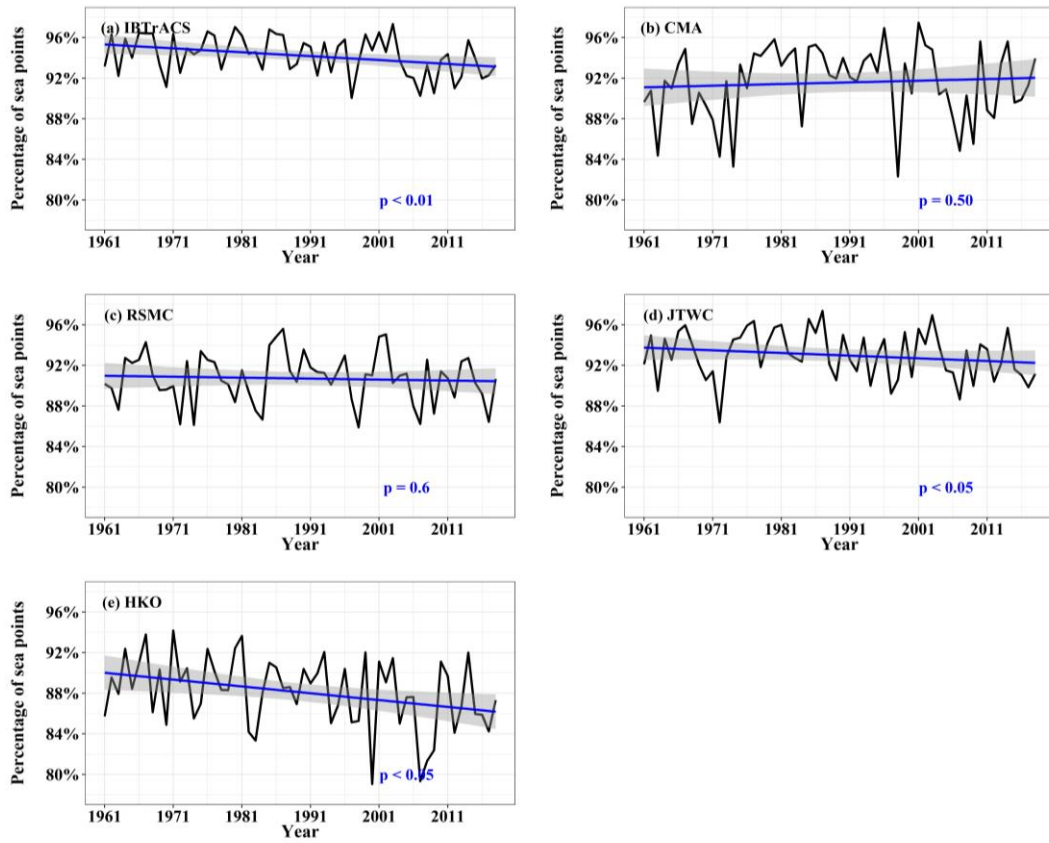


Fig. S18 Temporal changes in percentages of WNP TC position points over the sea to total numbers during 1961-2019 from the IBTrACS, CMA, RSMC, JTWC, and HKO datasets, respectively. The gray shadows are 95% confidence intervals of the linear trends.

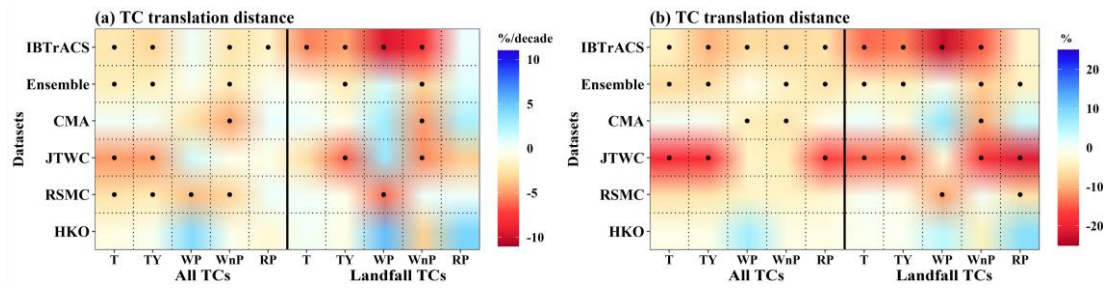


Fig. S19 Changes in TC translation distance over the WNP during 1981-2019. a is the long-term trends (units: %/decade) and b are the relative changes (units: %) between 1981-1997 (before the change point) and 1998-2019 (after the change point). The black dots indicate the changes at the 95% confidence level. T, TY, WP, WnP, and RP indicate total TCs, typhoons, west paths, west-north paths, and recurving paths, respectively. “Ensemble” indicates multi-dataset ensemble mean.

Table S1 Typhoon Khanun positions in the IBTrACS dataset and maximum sustained wind speeds in the four agencies.

Time	TC position in IBTrACS		Maximum sustained wind speed (Knot)			
	Lon (deg)	Lat (deg)	CMA	RSMC	JTWC	HKO
2005/9/5 0:00	142.3	8.2	23	-	-	-
2005/9/5 6:00	140.9571	8.628572	23	-	25	-
2005/9/5 12:00	139.9273	9.272727	23	-	30	-
2005/9/5 18:00	138.8333	10	29	-	35	-
2005/9/6 0:00	137.8308	10.52308	29	-	35	25
2005/9/6 6:00	136.76	10.98667	29	-	35	30
2005/9/6 12:00	136.025	12	29	-	40	30
2005/9/6 18:00	135.3	12.9	34	-	45	30
2005/9/7 0:00	134.425	13.525	34	35	45	35
2005/9/7 6:00	133.875	13.625	38	40	55	40
2005/9/7 12:00	133.55	14.025	48	45	55	45
2005/9/7 18:00	132.975	14.75	48	50	60	50
2005/9/8 0:00	132.5	15.35	54	55	65	55
2005/9/8 6:00	132.225	16.35	58	55	65	55
2005/9/8 12:00	131.525	17.375	64	60	65	55
2005/9/8 18:00	131.075	18.2	64	65	70	60
2005/9/9 0:00	130.425	19.175	77	80	75	60
2005/9/9 6:00	129.65	20.4	77	80	80	65
2005/9/9 12:00	128.5	21.4	77	80	90	70
2005/9/9 18:00	127.475	22.25	77	75	90	70
2005/9/10 0:00	126.275	23.2	87	75	95	75
2005/9/10 6:00	125.25	24.2	87	85	105	90
2005/9/10 12:00	124.425	25.125	97	85	110	90
2005/9/10 18:00	123.5	26.1	97	85	115	90
2005/9/11 0:00	122.7	27.275	97	80	110	90
2005/9/11 6:00	121.85	28.3	97	75	105	85
2005/9/11 12:00	120.9133	29.35333	64	65	80	70
2005/9/11 18:00	120.2692	30.48462	48	50	65	55
2005/9/12 0:00	119.4667	31.8	38	40	-	45
2005/9/12 6:00	119.3667	32.9	38	35	-	40
2005/9/12 12:00	120.0364	34.22727	38	35	-	35
2005/9/12 18:00	121.1	35.14445	34	35	-	30
2005/9/13 0:00	122.6	35.7	29	-	-	-
2005/9/13 6:00	124.8	36.4	29	-	-	-
2005/9/13 12:00	126.2	36.8	23	-	-	-

Note: Only TC positions with maximum sustained wind speed no less than 20 knots are shown. The bold values indicate that TC positions are confirmed by all the four agencies. The red values indicate that TC positions are extratropical transition which are not considered in our manuscript. “-” indicates no recorded values in the corresponding agencies.

Table S2 Spearman rank correlation between TC translation distance and TC generation and termination locations.

Dataset	Generation		Termination					
	Lat	Lon	WP.lat	WP.lon	WnP.lat	WnP.lon	RP.lat	RP.lon
IBTrACS	-0.72**	0.76**	0.13	0.02	0.32**	0.53**	0.46**	0.27**
CMA	-0.62**	0.65**	-0.06	0.09	0.30**	0.61**	0.21*	0.12
RSMC	-0.63**	0.73**	-0.02	0.06	0.17	0.52**	0.21*	0.20
JTWC	-0.44**	0.47**	-0.12	-0.04	0.14	0.42**	0.43**	0.30**
HKO	-0.59**	0.66**	0.11	-0.17	0.36**	0.54**	0.34**	0.29**

Note: “**/*” indicates the correlation is significant at the 0.05/0.1 level. “lon/lat” incates “longitude/latitude”. WP, WnP, and RP indicate west path, west-north path, and recurving path, respectively.

Table S3 The same as Table S2 but for the linear detrended TC translation distance and TC generation and termination locations.

Dataset	Generation		Termination					
	Lat	Lon	WP.lat	WP.lon	WnP.lat	WnP.lon	RP.lat	RP.lon
IBTrACS	-0.70**	0.74**	0.18	-0.04	0.39**	0.52**	0.46**	0.21*
CMA	-0.58**	0.64**	0.02	0.01	0.42**	0.63**	0.20	0.02
RSMC	-0.60**	0.73**	0.08	-0.05	0.24*	0.51**	0.19	0.12
JTWC	-0.42**	0.44**	-0.12	-0.05	0.14	0.42**	0.41**	0.25**
HKO	-0.65**	0.69**	0.01	-0.04	0.39**	0.53**	0.33**	0.26**